Supporting online information for: Anisotropy enhanced X-ray scattering from solvated transition metal complexes

Elisa Biasin,[a,b]* Tim B. van Driel,[a,f] Gianluca Levi,[c] Mads G. Laursen,[a] Asmus O. Dohn,[d] Asbjørn Moltke,[a] Peter Vester,[a] Frederik B. K. Hansen,[a] Kasper S. Kjær,[a,b,e] Tobias Harlang,[a] Robert Hartsock,[b] Morten Christensen,[a] Kelly J. Gaffney,[b] Niels E. Henriksen,[c] Klaus B. Møller,[c] Kristoffer Haldrup[a] and Martin M. Nielsen[a]

[a]*Department of Physics, Technical University of Denmark, Fysikvej 307, DK-2800 Kongens Lyngby, Denmark,* [b]*PULSE Institute, SLAC National Accelerator Laboratory, Menlo Park, California 94025, USA,* [c]*Department of Chemistry, Technical University of Denmark, Kemitorvet 207, DK-2800 Kongens Lyngby, Denmark,* [d]*Faculty of Physical Sciences, University of Iceland,* [e]*Department of Chemical Physics, Lund University, Box 118, S-22100 Lund, Sweden, and* [f]*Linac Coherent Light Source, SLAC National Accelerator Laboratory, Menlo Park, California 94025, USA. E-mail: elbia@fysiks.dtu.dk*

1. Additional Figures

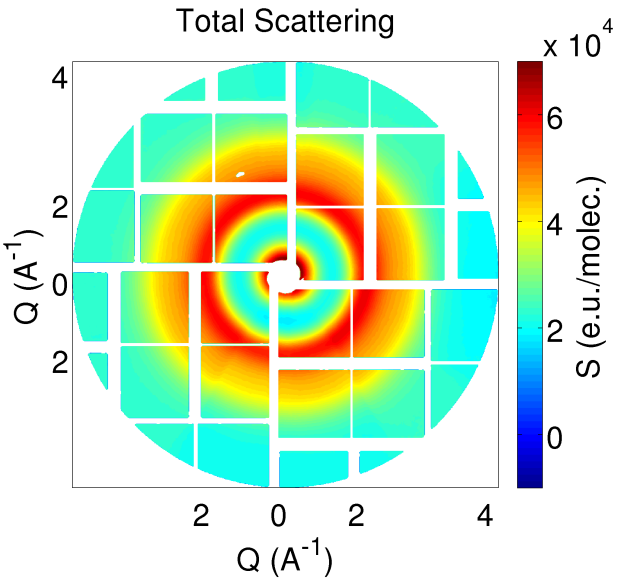

Fig. S1. Full X-ray scattering pattern arising from a 80 mM water solution of PtPOP, after corrections for X-ray polarization, solid angle coverage and masking. The magnitude of the difference scattering signal shown in the main article (Fig. 4b) is found $\sim$ 1 % of total scattering.

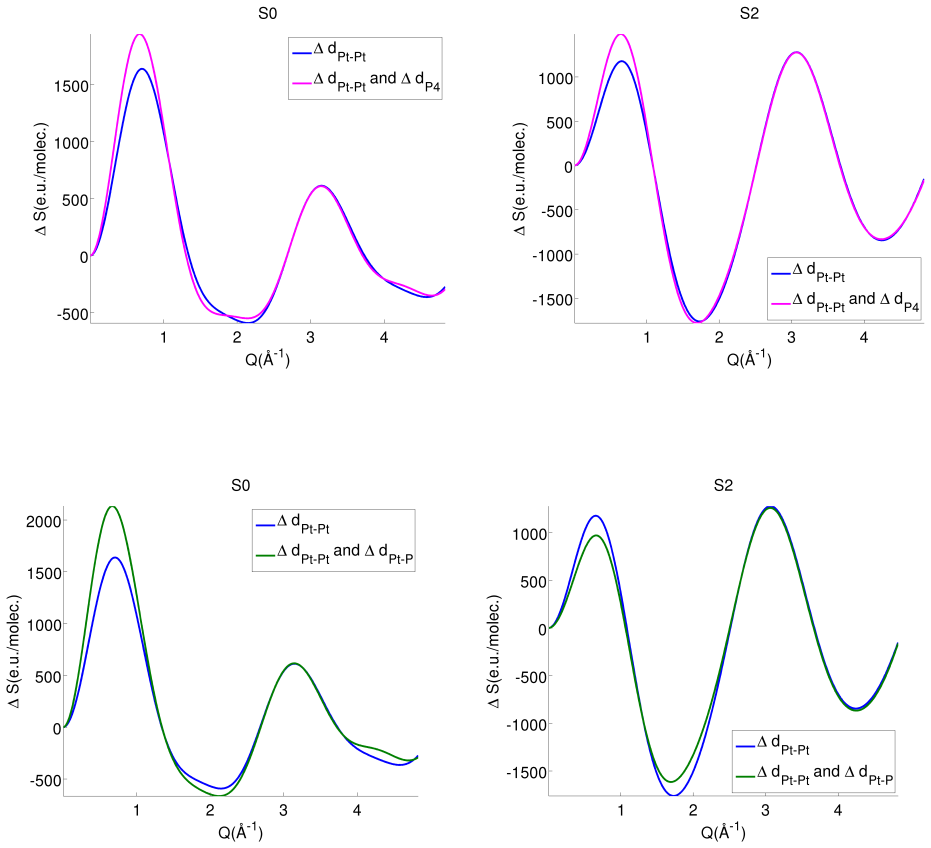

Fig. S2. **top)** Comparison between the isotropic (left) and anisotropic (right) difference scattering signals arising from a 0.25 Å contraction of the Pt-Pt bond (blue line) and from this contraction with an additional 0.04 Å contraction of the four-phosphorous planes (magenta line). This additional deformation involves mostly changes of intra-molecular distances that are parallel to the Pt-Pt axis and add a positive contribution to both the isotropic and anisotropic difference scattering signal. **bottom)** Comparison between the isotropic (left) and anisotropic (right) difference scattering signals arising from a 0.25 Å contraction of the Pt-Pt bond (blue line) and from this contraction with an additional 0.02 Å contraction of each Pt-ligand distance (green line). This additional deformation involves mostly changes of intra-molecular distances that are perpendicular to the Pt-Pt axis and add a positive contribution to the isotropic difference scattering signal and a negative contribution to the anisotropic signal, accordingly to Eq.10.

2. DFT calculations in vacuum

The set of molecular structures used to simulate the solute difference scattering signal (ΔS^{solute}) was obtained from a DFT-optimized geometry of ground state PtPOP by varying the Pt-Pt distance from 2.700 to 3.300 Å in steps of 0.001 Å while keeping all the other atoms fixed.

The geometry optimization was performed in the Atomic Simulation Environment (Bahn & Jacobsen, 2002; Larsen *et al.*, 2017) and employing the Grid-based Projector Augmented Wave (GPAW) DFT code (Mortensen *et al.*, 2005; Enkovaara *et al.*, 2010). The exchange-correlation functional was BLYP (Becke, 1988; Lee *et al.*, 1988), while a linear combination of atomic orbitals (LCAO) with tzp basis for Pt and dzp for the rest of the atoms was used to represent the Kohn-Sham wave functions (Larsen *et al.*, 2009). We employed a grid spacing of 0.18 Å. The geometry was optimized until the maximum force on all individual atoms was less than 0.02 eV/Å. A vibrational analysis using the finite difference method implemented in ASE was carried out on the optimized geometry to confirm that it is a true minimum of the potential energy surface. The resulting structure has approximate C_{4h} symmetry, and features a Pt-Pt distance of 3.005 Å. In comparison, the values found from X-ray crystallographic studies lie in the range 2.913-2.979 Å (Pinto *et al.*, 1980; Che *et al.*, 1983; Ozawa *et al.*, 2003; Yasuda *et al.*, 2004), while previous X-ray diffraction measurements in water solution delivered a Pt-Pt distance of 2.98 Å (Christensen *et al.*, 2008).

3. Simulation of ΔS^{cage} and $\Delta S^{solvent}$

ΔS^{cage} in Eq.15 is calculated from solute-solvent RDFs of QM/MM simulations performed in the ground and excited states, as detailed in the next section, and following the procedure described by Dohn *et al.* (Dohn *et al.*, 2015). $\Delta S^{solvent}$ in Eq.15 is

calculated as following:

$$\Delta S^{solvent}(Q) = \Delta T \frac{\partial S(Q)}{\partial T}\bigg|_{\rho}. \tag{S1}$$

where ΔT is the change in temperature and $\frac{\partial S(Q)}{\partial T}\Big|_{\rho}$ is the water solvent differential, that was measured in separate experiment and archived (Kjær *et al.*, 2013; Sørensen & Kjær, 2013). The fit of Eq.15 to the isotropic scattering signal in Fig.5(right) yields $\beta \sim 1.9$ % and $\Delta T \sim 0.28$ K.

4. QM/MM MD simulations

The solute-solvent RDFs for PtPOP in water were obtained from a previous QM/MM Born-Oppenheimer Molecular Dynamics (BOMD) investigation (Dohn *et al.*, 2017). The DFT level of theory and atomic orbital basis set used to the describe the complex were the same as those utilized here for the geometry optimization in vacuum. The ground state RDFs were calculated from 230000 MD frames spanning a total simulation time of around 460 ps. A detailed account of the QM/MM interfacing strategy, MM force field and MD protocol that were used in the QM/MM BOMD simulations is provided in (Dohn *et al.*, 2017). To compute the RDFs for PtPOP in the first singlet excited state, 99 excited-state QM/MM trajectories were started from uncorrelated frames of the equilibrium ground state trajectories collected in (Dohn *et al.*, 2017). In these simulations the excited state was described with a modified version of ΔSCF (Ziegler *et al.*, 1977) in the spin unpolarized formalism (Maurer & Reuter, 2011; Himmetoglu *et al.*, 2012). The method uses Gaussian smeared constraints of the orbitals occupation numbers (Maurer & Reuter, 2011) to achieve stable convergence of the density at each step of the dynamics and is implemented in a local version of GPAW. Time step and thermostatting scheme were the same as those used for the ground state equilibrium simulations in (Dohn *et al.*, 2017). Equilibrium excited-state RDFs were calculated from around 80000 MD snapshots, corresponding to 160 ps remaining

after having removed the non-equilibrated part of each trajectory.

References

Bahn, S. R. & Jacobsen, K. W. (2002). *Computing in Science & Engineering*, **4**, 55.

Becke, A. D. (1988). *Physical Review A*, **38**, 3098.

Che, C. M., Herbstein, F. H., Schaefer, W. P., Marsh, R. E. & Gray, H. B. (1983). *Journal of the American Chemical Society*, **105**(14), 4604–4607.

Christensen, M., Haldrup, K., Bechgaard, K., Feidenhans, R., Kong, Q., Cammarata, M., Russo, M. L., Wulff, M., Harrit, N., Nielsen, M. M., Kong, Q., Cammarata, M., Russo, M. L. & Wulff, M. (2008). *J. Am. Chem. Soc*, **131**(Ii), 502–508.

Dohn, A. O., Biasin, E., Haldrup, K., Nielsen, M. M., Henriksen, N. E. & Møller, K. B. (2015). *Journal of Physics B: Atomic, Molecular and Optical Physics*, **48**, 244010.

Dohn, A. O., Jonsson, E. Ö., Levi, G., Mortensen, J. J., Lopez-Acevedo, O., Thygesen, K. S., Jacobsen, K. W., Ulstrup, J., Henriksen, N. E., Møller, K. B. & Jonsson, H. (2017). *J. Chem. Theory Comput.* **JustAccepted**.

Enkovaara, J., Rostgaard, C., Mortensen, J. J., Chen, J., Dulak, M., Ferrighi, L., Gavnholt, J., Glinsvad, C., Haikola, V., Hansen, H. A., Kristoffersen, H. H., Kuisma, M., Larsen, A. H., Lehtovaara, L., Ljungberg, M., Lopez-Acevedo, O., Moses, P. G., Ojanen, J., Olsen, T., Petzold, V., Romero, N. A., Stausholm-Møller, J., Strange, M., Tritsaris, G. A., Vanin, M., Walter, M., Hammer, B., Häkkinen, H., Madsen, G. K. H., Nieminen, R. M., Nørskov, J. K., Puska, M., Rantala, T. T., Schiøtz, J., Thygesen, K. S. & Jacobsen, K. W. (2010). *Journal of Physics: Condensed matter*, **22**, 253202.

Himmetoglu, B., Marchenko, A., Dabo, I. & Cococcioni, M. (2012). *Journal of Chemical Physics*, **137**(15), 154309.

Kjær, K. S., van Driel, T. B., Kehres, J., Haldrup, K., Khakhulin, D., Bechgaard, K., Cammarata, M., Wulff, M., Sørensen, T. J. & Nielsen, M. M. (2013). *Physical Chemistry Chemical Physics*, **15**, 15003–15016.

Larsen, A. H., Mortensen, J. J., Blomqvist, J., Castelli, I. E., Christensen, R., Duak, M., Friis, J., Groves, M. N., Hammer, B., Hargus, C., Hermes, E. D., Jennings, P. C., Jensen, P. B., Kermode, J., Kitchin, J. R., Kolsbjerg, E. L., Kubal, J., Kaasbjerg, K., Lysgaard, S., Maronsson, J. B., Maxson, T., Olsen, T., Pastewka, L., Peterson, A., Rostgaard, C., Schitz, J., Schtt, O., Strange, M., Thygesen, K. S., Vegge, T., Vilhelmsen, L., Walter, M., Zeng, Z. & Jacobsen, K. W. (2017). *Journal of Physics: Condensed Matter*, **29**(27), 273002.

Larsen, A. H., Vanin, M., Mortensen, J. J., Thygesen, K. S. & Jacobsen, K. W. (2009). *Phys. Rev. B*, **80**, 195112.

Lee, C., Yang, W. & Parr, R. G. (1988). *Physical Review B*, **37**, 785–789.

Maurer, R. J. & Reuter, K. (2011). *Journal of Chemical Physics*, **135**(22), 224303.

Mortensen, J., Hansen, L. & Jacobsen, K. W. (2005). *Physical Review B*, **71**, 035109.

Ozawa, Y., Terashima, M., Mitsumi, M., Toriumi, K., Yasuda, N., Uekusa, H. & Ohashi, Y. (2003). *Chemistry Letters*, **32**(1), 62–63.

Pinto, M. A. F. D. R., Sadler, P. J., Neidle, S., Sanderson, M. R., Subbiah, A. & Kuroda, R. (1980). *J. Chem. Soc., Chem. Commun.* pp. 13–15.

Sørensen, T. J. & Kjær, K. S., (2013). Https://sites.google.com/site/trwaxs/.

Yasuda, N., Uekusa, H. & Ohashi, Y. (2004). *Bulletin of the Chemical Society of Japan*, **77**(5), 933–944.

Ziegler, T., Rauk, A. & Baerends, E. J. (1977). *Theoretica Chimica Acta*, **43**(3), 261–271.